Holocene elemental, lead isotope and charcoal record from peat in southern Poland

K. Tudyka[1], A. Pazdur[1], F. De Vleeschouwer[2], M. Lityńska-Zając[3], L. Chróst[4] and N. Fagel[5]

[1] Department of Radioisotopes, Institute of Physics, Silesian University of Technology, Gliwice, Poland
[2] University of Toulouse (INP, UPS) and CNRS, EcoLab, ENSAT, Castanet Tolosan, France
[3] Institute of Archaeology and Ethnology, Polish Academy of Sciences, Kraków, Poland
[4] Laboratory for Ecological Research, Measurement and Expertise, Gliwice, Poland
[5] UR AGEs, Department of Geology, University of Liège (Sart Tilman), Belgium

SUMMARY

This article presents a mid-resolution elemental, isotopic and charcoal record from 10700 BC to AD 500 in a peat core located in Żyglin (southern Poland). The objective is to give insight into the proxies with emphasis on lead (Pb) sources in this minerogenic peat deposit. During the Early Holocene (10700–7550 BC) the average $^{206}Pb/^{207}Pb$ quotient was around 1.196. This isotopic signature is consistent with natural dust derived from long-distance soil and rock weathering. The Mid-Holocene period (7550–3200 BC) shows a significant change in the peat accumulation conditions. The growth rate is approximately 0.04 mm yr^{-1} and the $^{206}Pb/^{207}Pb$ quotients are shifted toward values that are found in local galena ores. This is simultaneous with a significantly increased lead flux which further confirms local sources of material in this peat deposit. In the Late Holocene period (3200 BC–AD 500) a large quantity of charcoal particles with diameters ranging from 2 mm up to 3 cm is found; also, Pb, Zn and Cu fluxes reach their highest values. This period corresponds to the Eneolithic, Bronze and Iron Ages, and human impact is recorded as charcoal.

KEY WORDS: age-depth model, chronology, geochemistry, $^{206}Pb/^{207}Pb$, radiocarbon dating, Silesia

INTRODUCTION

Upper Silesia in southern Poland (Figure 1, A and B) is characterised by abundant lead, zinc and silver deposits that have been mined in the past. For example, the town Tarnowskie Góry was a lead and silver mining centre during the 16th century and it is estimated that about 20,000 small mine shafts existed in the area (Drabina 2000). During that time large quantities of ore deposits were still easily accessible on the surface. Earlier signs of human activity such as a hill fort from the Bronze Age and four other populated locations dating back to the Bronze and Iron Ages are reported in Tarnowskie Góry County (NID 2014). In the National Heritage Board of Poland undisclosed archives, 12 archaeological sites ranging from Stone Age to Iron Age are reported in the same region (NID 2014). Despite these findings, the timeframe and geographical extent of Upper Silesian metallurgy is still relatively unknown. This is mainly due to the lack of artefacts that would attest to ancient mining or smelting centres. In Poland the beginning of the Bronze Age is estimated at 2300–2000 BC and the beginning of the Iron Age to 1000–700 BC. Preliminary studies (Chróst *et al*. 2007, 2008; Chróst 2013) of minerotrophic peat cores from Silesia suggested that smelting could have begun between the 9th and 11th centuries AD. However, those studies also pointed out the confusing data. Indeed, significant amounts of charcoal and lead were found in the older peat layers and remained unexplained. The preliminary studies lacked a good chronology, which is crucial to constraining the history of human activity in this region. The recent studies conducted on the same peat deposits by Cabala *et al*. (2013) and Magiera *et al*. (2016) confirmed Common Era human activities in Silesia. In the Cabala *et al*. (2013) work, unexpected Zn-Cu and Ag-Au alloys were reported in the peat layers corresponding to older prehistoric times.

Peat profiles and cores are a good alternative to archaeological investigation because they are valuable archives of climatic and anthropic impacts (e.g. Weiss *et al*. 1999, Lamentowicz *et al*. 2009). Ombrotrophic peat deposits have proved to be reliable for reconstructing historical metal pollution (Shotyk *et al*. 1998, Renson *et al*. 2008, De Vleeschouwer *et al*. 2009, 2012) but, unfortunately, they are virtually absent from the investigated region. Some previous studies (Shotyk *et al*. 2000, Baron *et al*. 2005) have successfully used

 DOI: 10.19189/MaP.2016.OMB.257

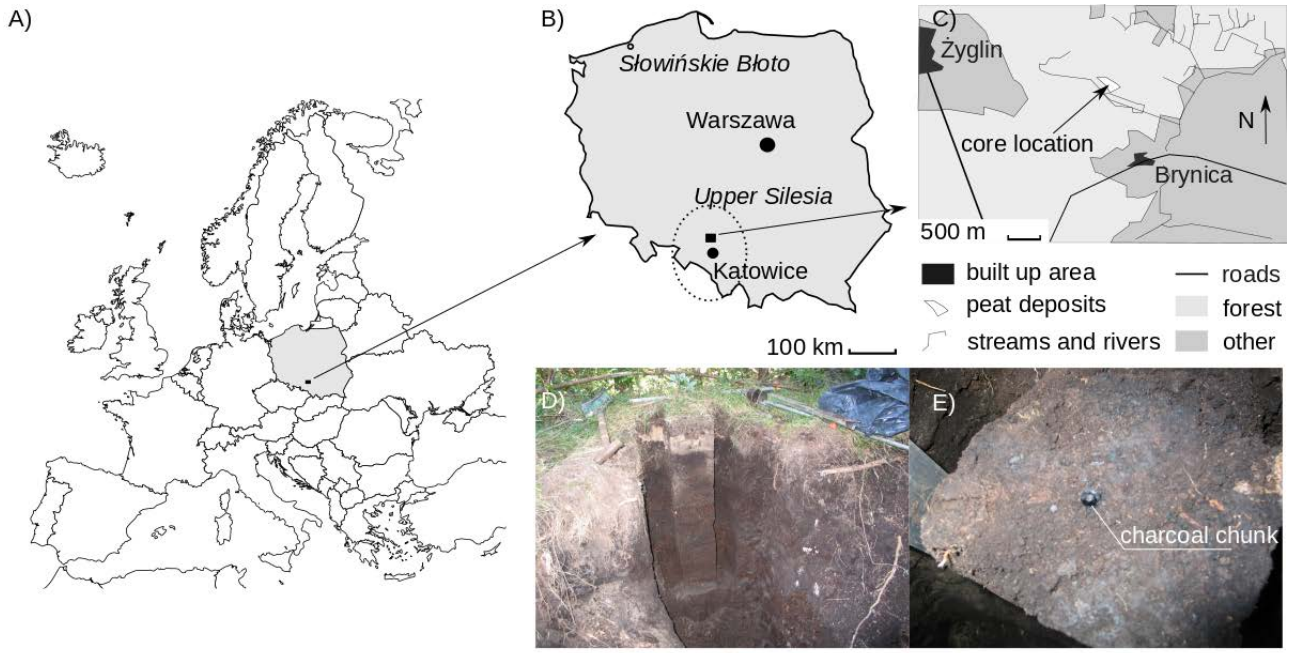

Figure 1. A), B) and C) site location, D) peat core photo, E) charcoal in the peat profile.

minerotrophic peat profiles to reconstruct anthropogenic contamination. In these studies, lead concentrations are higher in the surface and sub-surface layers and decrease significantly with depth. While careful interpretation is needed, owing to possible post-depositional elemental mobility (Novak & Pacherova 2008), the use of minerotrophic peat nevertheless gives the opportunity to investigate early human activity in Upper Silesia.

The ore deposits in Silesia are hosted mainly in the Silesia-Cracow monocline of southern Poland. The monocline contains Triassic, Jurassic and Cretaceous rocks. Sulphide deposits, which consist largely of sphalerite, galena and iron sulphides, typically have stratabound and tabular forms (Leach & Viets 1992, 1993).

This study aims to investigate the elemental and isotopic content as well as the charcoal abundances of a minerotrophic peat core from Żyglin, Upper Silesia. The combination of proxies is used in order to: (1) reconstruct metal (Pb, Zn, Ti and Cu) and charcoal fluxes in the record; (2) link this to known periods of climatic, local environmental and human induced changes in the proxies with the help of radiocarbon dating; and (3) identify the possible provenance of trace metals with lead isotopes.

METHODS

Peat sampling

The material was collected near Żyglin (see B and C in Figure 1) in Upper Silesia (southern Poland). The peat deposit in Żyglin has a triangular shape and was drained twice, during the inter-war period (1918–1939) and in the 1980s. It covers an area of more than 2 ha and is situated near the drainage basin of the Brynica River (Figure 1C). Owing to a 20 cm sand layer covering the surface, the fen is preserved and allows investigation (Figure 1D).

Three peat monoliths were taken from the same location (249 m above mean sea level) to provide sufficient material for the investigations. The co-ordinates from which the cores were retrieved are 50° 28′ 56.20″ N, 18° 59′ 12.19″ E. The total length of the cores was 130 cm. In the uppermost 20 cm section they were mainly composed of sand and the remaining 110 cm was composed of fen peat. Monoliths were taken near the drainage ditch after removing approximately 1.5 m of the peat to reach areas where our proxies were not affected by the ditch (Figure 1D). Monoliths were wrapped in plastic film and stored in PVC tubes for transport. In the laboratory, peat cores were stored at 4 °C in the refrigerator before subsampling.

^{14}C dating

Samples were treated with a standard Acid-Alkali-Acid procedure to remove humic acids, chitin, fungal products, carbonates, *etc*. Next, the samples were converted to C_6H_6 and stored for more than one month to allow all ^{222}Rn isotopes to decay. After that, butyl-PBD was added to 2 ml of C_6H_6. A more detailed description of procedures, precision and accuracy obtained in the GADAM Centre laboratory in Gliwice is provided by Pawlyta *et al*. (1998).

 DOI: 10.19189/MaP.2016.OMB.257

Liquid scintillation measurements were performed with one Quantulus 1220™ and two ICELS spectrometers (Theodórsson 2005, Tudyka & Pazdur 2012) equipped with the additional multichannel analyser Tukan 8k. The radiocarbon dates were calculated according to Stuiver & Polach (1977).

In this work, radiocarbon dates from Table A1 (Appendix) reported earlier by Tudyka & Pazdur (2010, 2012) from three liquid scintillation counting spectrometers were combined using the weighted mean from each peat layer. This allowed us to create a more accurate and precise time scale than previously. The ^{14}C dates were calibrated with the IntCal13 (Reimer *et al*. 2013) curve and the age-depth model (Figure 2) was retrieved using OxCal v4.2.2 software (Bronk Ramsey 2009) with built-in P_Sequence(2) function (Bronk Ramsey 2008). In the age-depth model three samples from depths 20–21 cm, 29–30 cm and 92.5–95 cm were identified as possible outliers and, therefore, rejected. The model obtained was used to calculate the accumulation rate.

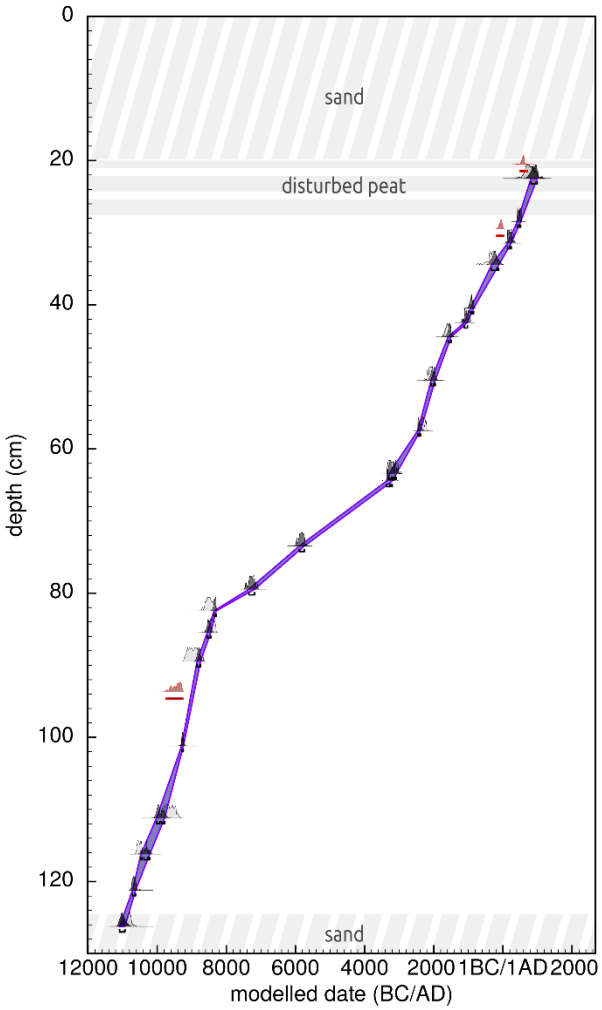

Figure 2. Age-depth model obtained with weighted mean of results from one Quantulus 1220™ and two ICELS systems. Purple curve presents 68 % highest probability density range. Distributions for the single weighted calibrated dates are marked with light grey. Posterior distributions are marked with dark grey which takes into account the age-depth model. The outliers are marked in red.

Elemental geochemistry

Dry samples selected for the elemental geochemistry were crushed manually using a clean agate pestle and mortar, which were rinsed between each sample using mQ water and *p.a.* grade ethanol. The samples were then stored in 20 ml plastic vials. Approximately 100 mg of dried and homogenised peat powder was weighed out and digested in a PTFE beaker in a clean room equipped with class 100 flow benches at EcoLab (Toulouse, France). All acids used were of ultrapure quality. The digestion procedure consisted of three steps. Each step was succeeded by a slow evaporation at 55 °C (Le Roux & De Vleeschouwer 2010): (1) a mixture of 0.5 ml HF and 2 ml 16 M HNO_3 was added and left on the hotplate at 110 °C for two days; (2) 1 ml of H_2O_2 was added to react for six hours at room temperature; (3) 2 ml of 16 M HNO_3 was added and left at 90 °C for two days to finalise the digestion. The samples were subsequently dissolved in 2 ml of 35 % HNO_3, transferred into 15 ml polypropylene tubes and further diluted with mQ water up to 14 ml. All samples were preserved in a refrigerator for future analyses. After proper dilution the concentration of selected elements (Al, Ca, Cu, Fe, Mg, Mn, Na, P, Pb, S, Sr, Ti, Zn) was measured on an inductively coupled plasma optical emission spectrometer (ICP-OES) manufactured by Thermo Scientific (IRIS Intrepid II). Measurements were performed at EcoLab (Toulouse, France). The ICP-OES was calibrated using a synthetic multi-element standard. The accuracy of the analyses was assessed by the analysis of two internationally certified reference materials (BCR142-lichen and NIMT-peat).

Lead isotopic analyses

According to the measured lead concentration in each sample, a variable amount of dry peat powder was taken in order to obtain 2,000 ng of Pb in the final solution dedicated to the isotopic analysis. The peat samples were firstly combusted (550 °C, 4 h) and then digested in 4 ml HF 24 N + 1 ml HNO_3 14 N in PTFE beakers (120 °C, 48 h) in class 1000

laminar flow clean air cabinets (AGEs, University of Liège, Belgium). After complete evaporation, 1 ml of 6 N HCl was added and the solutions were slowly evaporated. Dried residues were dissolved in 0.8 N HBr before chromatographic separation. Lead was separated using preconditioned anionic resin (AG1X8) in exchange micro-columns by successive HCl and HBr additions (Weis *et al*. 2005). The eluted pure Pb solution was evaporated and stored. Before the isotopic analysis the Pb elution was re-dissolved in 100 µl of 14 N HNO_3, evaporated and finally dissolved in 1.5 ml of 0.05 N HNO_3. Lead isotopic quotients were measured on a Nu Instruments Multi-Collector Inductively Coupled Plasma Mass Spectrometer (MC-ICP-MS) at the Laboratoire G-Time (Université Libre de Bruxelles, Belgium). The configuration of the collector array enabled a simultaneous collection of Pb (for masses 208, 207, 206, 204), Tl (205, 203) and Hg (202). Mercury (Hg) was used to correct interferences on mass 204 (because of ^{204}Hg). Thallium (T1) was added to all samples and standards to monitor and correct instrumental mass fractionation. All the standard and sample solutions were prepared to obtain a Pb/Tl quotient of ~ 5, a signal of ~100 mV on the axial collector ^{204}Pb, and to match the Pb and Tl concentrations of the standards (200 ng g^{-1} and 50 ng g^{-1}, respectively). The NBS981 provided regular checks of reproducibility and drift during each day. The details about MC-ICP-MS tuning and calibration for this type of sample are reported by De Vleeschouwer *et al*. (2007). The Pb background of the blank sample is 7 ng.

Charcoal content and charcoal taxonomical identification

Charcoal fragments were carefully separated by hand from the large cross section (20 × 20 cm) peat core. After drying, the mass of charcoal was measured and the mass of charcoal *per* unit peat volume was calculated.

The charcoal conserves the anatomical structure of the wood, and this permits its botanical identification. Within the separate sub-core 1,176 charcoal pieces were found. From these, 686 pieces with longest dimension > 2 mm were selected for taxonomical identification. Each charcoal fragment was broken to expose transverse, longitudinal tangential and longitudinal radial sections under a reflected light stereomicroscope. The microscope was manufactured by Nikon and 100–500 × magnification was used for the taxonomical identification. The investigated charcoal was compared with modern reference material in the Institute of Archaeology and Ethnology of the Polish Academy of Sciences, as well as with literature (Schweingruber 1978, 1990; Lityńska-Zając & Wasylikowa 2005).

RESULTS

The age-depth model (Figure 2) allowed us to assign a time scale to the elemental geochemistry (Figure 3, Table 1), lead isotopes (Figures 4 and 5, Table 2), charcoal mass *per* unit of peat volume (Table 3) and charcoal taxonomical identification (Figure 6, Table 4). In each Table and for each peat layer, the calendar age from the age-depth model is given. In Table 1, which shows the elemental geochemistry content, the accuracy of the measurement is also reported, except for P, S and Sr, which are not certified in the reference materials.

The size range of the charcoal pieces reported in Table 3 is from 2 mm up to 3 cm (Figure 1E). The charcoal content dataset is semi-quantitative because it is possible that the charcoal was not spread uniformly across the peat area. This could have happened, for example, if charcoal had been delivered preferentially to some parts of the peat area because of water flow or human activity. The assemblage of charcoal pieces is not equi-dimensional; it comprises a variety of sizes. This may imply minimal transport (Nichols *et al*. 2000, Scott 2010). The number of charcoal pieces in taxonomical identification for a given peat layer may not be a representative measure for the entire peat area. In other words, pieces could be crushed,

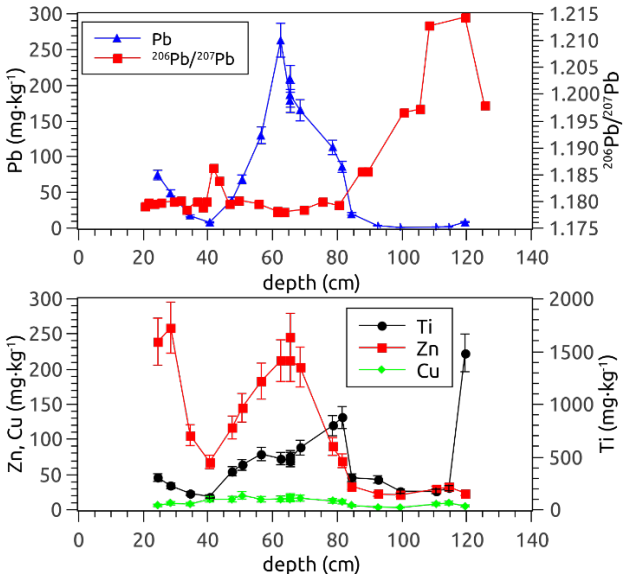

Figure 3. Pb, ^{206}Pb/^{207}Pb, Ti, Zn and Cu proxies *versus* peat depth.

Table 1. Elemental geochemistry measurements on selected peat samples from Żyglin 3 core. Notes: [a] the entire procedure was replicated for the 65–66 cm sample; [b] second analysis of the 65–66 cm sample; [c] accuracy is assigned for concentrations of elements in the corresponding columns except for P, S and Sr, which were not certified in the reference materials used.

Depth (cm)	Peat layer boundaries calibrated mean age	Al (mg kg^{-1})	Ca (mg kg^{-1})	Cu (mg kg^{-1})	Fe (mg kg^{-1})	Mg (mg kg^{-1})	Mn (mg kg^{-1})	Na (mg kg^{-1})	P (mg kg^{-1})	Pb (mg kg^{-1})	S (mg kg^{-1})	Sr (mg kg^{-1})	Ti (mg kg^{-1})	Zn (mg kg^{-1})
24–25	AD 796 – AD 723	4700	13285	6.3	11064	407	64.7	168	740	74.4	2012	51.2	305	239
28–29	AD 504 – AD 422	5004	17405	9.12	10974	476	91.5	151	902	49.2	2591	64.1	227	259
34–35	163 BC – 290 BC	4523	15328	8.09	8504	414	93	106	707	17.2	2414	53.9	155	106
40–41	846 BC – 945 BC	4460	17008	15	9190	393	108	59.9	549	8.17	2355	58.4	126	68
47–48	1742 BC – 1822 BC	5769	14868	15.1	9340	506	88.3	294	1028	39.7	2997	53.9	365	117
50–51	1984 BC – 2052 BC	5793	11978	20.6	10431	536	132	515	950	68.4	2476	50.4	425	145
56–57	2328 BC – 2383 BC	6459	14852	14.9	11609	697	141	568	968	130	3031	58.7	528	183
62–63	2991 BC – 3120 BC	6210	13119	15.5	13383	623	147	433	892	263	2874	54.1	485	212
65–66	3435 BC – 3717 BC	6148	13023	15.5	11971	596	124	491	845	178	2734	53.1	463	212
65–66 [a]	3435 BC – 3717 BC	6309	15304	17.9	13769	662	141	385	1007	209	3235	59	501	245
65–66 [b]	3435 BC – 3717 BC	5919	13402	16.7	12456	633	141	477	833	186	2820	54.8	485	212
68–69	4280 BC – 4561 BC	6367	13231	16.5	11125	653	140	710	782	165	2758	56	588	203
78–79	6918 BC – 7160 BC	7222	16665	12.5	11483	1211	139	620	818	113	3458	64.2	797	90
81–82	7807 BC – 8159 BC	7529	15990	11.2	10312	1074	138	777	804	85.8	3373	61.7	874	69.7
84–85	8417 BC – 8473 BC	5083	15128	5.86	7147	644	117	194	744	20	3796	49	304	33.5
92–93	8887 BC – 8929 BC	4533	15727	3.92	7190	731	90.3	199	669	3.41	3325	49.8	288	22.4
99–100	9177 BC – 9218 BC	3835	14667	3.27	7494	557	75	116	573	1.1	3684	44.7	176	21.3
110–111	9823 BC – 9887 BC	3994	14317	8.13	10870	539	76.1	116	594	1.66	5229	45.1	174	29.4
114–115	10137 BC – 10222 BC	4472	11644	9.56	10305	488	63.6	140	703	2.03	8193	37	205	32.4
119–120	10515 BC – 10583 BC	5644	6455	5.49	8175	935	76.8	1561	213	8.6	3073	34.3	1487	23.7
Accuracy (%) [c]		*11*	*25*	*26*	*23*	*18*	*18*	*14*		*9*			*12*	*14*

 DOI: 10.19189/MaP.2016.OMB.257

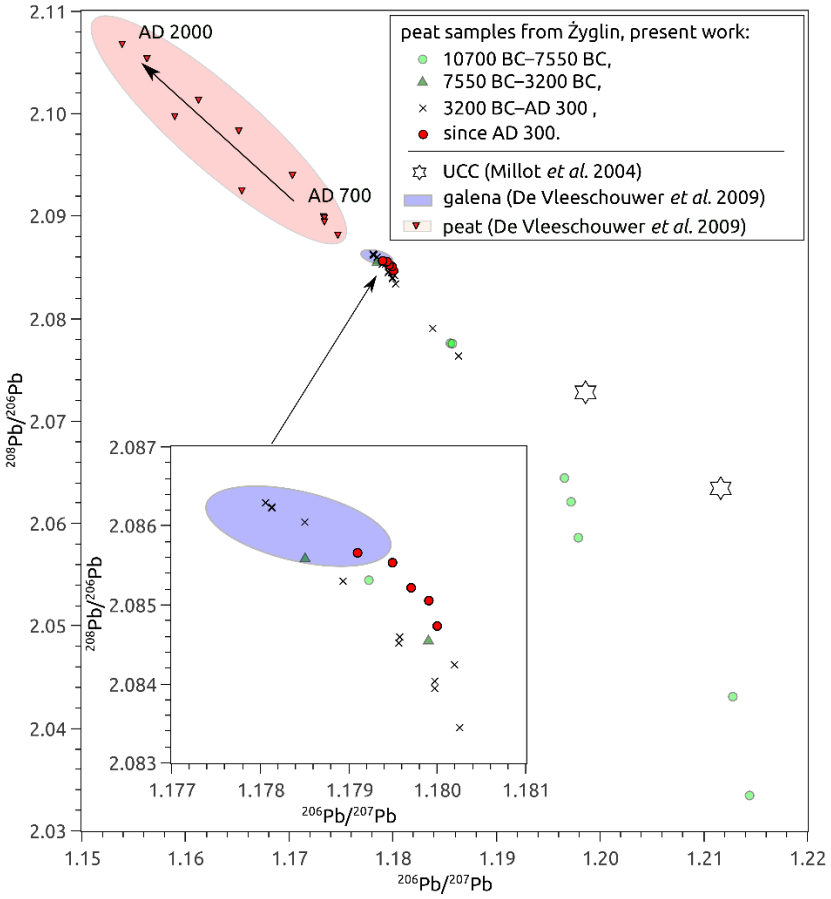

Figure 4. $^{208}Pb/^{206}Pb$ *versus* $^{206}Pb/^{207}Pb$ plot for: 23 samples from Żyglin (this work); 11 ombrotrophic peat samples (700 AD–2000 AD) (De Vleeschouwer *et al*. 2009); 11 galena samples from Chrzanów, Olkusz, Pomorzany (De Vleeschouwer *et al*. 2009); and Upper Continental Crust (UCC) estimated by Millot *et al*. (2004). The error bars are significantly smaller than the symbols.

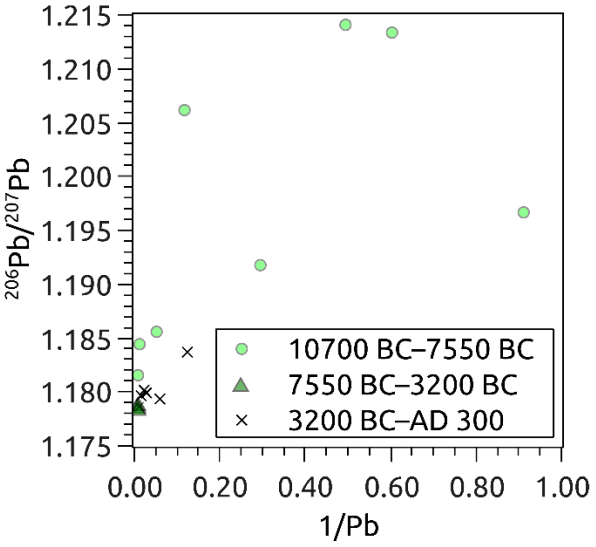

Figure 5. 1/Pb *versus* $^{206}Pb/^{207}Pb$ binary diagram, distinguishing the three periods discussed in this article. $^{206}Pb/^{207}Pb$ quotient was interpolated from the data in Table 2, then merged with Pb content from Table 1.

transported, *etc*. Hence, the frequency is qualitative information. Table 4 contains the results for 5-cm layers where the presence of charcoal is marked by a "+" symbol. These results are plotted in Figure 6, which shows relative frequencies of charcoal taxonomical identification plotted on a calendar time scale.

The elemental geochemistry (Figure 3, Table 1) can be presented more adequately for data analyses by calculating the flux of the element, which should ideally be immobile. An advantage of this approach is that the delivered mass of a certain element *per* unit area *per* year is obtained; that is, the element supply rate can be read directly from the flux. The flux was calculated from the mean density of the peat used (0.14 g cm^{-3}) with an uncertainty of approximately 10 %. The differences in density of the peat were very small because the peat area is covered with 20 cm of sand that has uniformly compressed the peat. The fluxes of the elements that were assumed to be immobile are presented on a calendar time scale in Figure 7. Another approach

Table 2. Lead isotopic quotient measurements on selected peat samples from Żyglin 3 core. 2σ uncertainty is given. * indicates a replicate.

Depth (cm)	Peat layer mean age range from the age-depth model	$^{208}Pb/^{204}Pb$	$^{207}Pb/^{204}Pb$	$^{206}Pb/^{204}Pb$	$^{208}Pb/^{206}Pb$	$^{206}Pb/^{207}Pb$
20–21	AD 1088 – AD 1015	38.4186 ± 0.0026	15.62098 ± 0.00080	18.41930 ± 0.00084	2.085661 ± 0.000044	1.179123 ± 0.00018
21–22	AD 1015 – AD 942	38.4368 ± 0.0026	15.62467 ± 0.00099	18.43253 ± 0.00086	2.085218 ± 0.000042	1.179695 ± 0.00018
23–24	AD 869 – AD 796	38.4287 ± 0.0020	15.6226 ± 0.00078	18.42661 ± 0.00096	2.085530 ± 0.000040	1.179457 ± 0.00016
25–26	AD 723 – AD 650	38.4329 ± 0.0014	15.62246 ± 0.00060	18.43266 ± 0.00060	2.085069 ± 0.000040	1.179861 ± 0.00020
29–30	AD 422 – AD 331	38.4373 ± 0.0024	15.62458 ± 0.00060	18.43760 ± 0.00082	2.084719 ± 0.000046	1.180030 ± 0.00020
31–32	AD 240 – AD 123	38.4305 ± 0.0026	15.62283 ± 0.00098	18.4384 ± 0.00010	2.084247 ± 0.000046	1.180233 ± 0.00016
33–34	20 BC – 163 BC	38.3988 ± 0.0018	15.61978 ± 0.00062	18.40771 ± 0.00062	2.086049 ± 0.000044	1.178488 ± 0.00014
36–37	401 BC – 512 BC	38.4174 ± 0.0022	15.62325 ± 0.00082	18.43483 ± 0.00086	2.083942 ± 0.000046	1.179979 ± 0.00022
38–39	623 BC – 735 BC	38.4088 ± 0.0018	15.62310 ± 0.00064	18.41874 ± 0.00080	2.085295 ± 0.000042	1.178941 ± 0.00016
39–40	735 BC – 846 BC	38.4183 ± 0.0022	15.62286 ± 0.00076	18.43459 ± 0.00088	2.084037 ± 0.000042	1.179972 ± 0.00014
41–42	945 BC – 1032 BC	38.5148 ± 0.0018	15.63591 ± 0.00064	18.54928 ± 0.00082	2.076367 ± 0.000038	1.186319 ± 0.00012
43–44	1192 BC – 1424 BC	38.4728 ± 0.0018	15.63036 ± 0.00064	18.50459 ± 0.00070	2.079062 ± 0.000042	1.183899 ± 0.00016
46–47	1661 BC – 1742 BC	38.4131 ± 0.0016	15.62261 ± 0.00056	18.42779 ± 0.00076	2.084518 ± 0.000044	1.179560 ± 0.00020
49–50	1903 BC – 1984 BC	38.4186 ± 0.0016	15.62343 ± 0.00066	18.43954 ± 0.00070	2.083439 ± 0.000050	1.180248 ± 0.00020
55–56	2273 BC – 2328 BC	38.4145 ± 0.0024	15.62187 ± 0.00080	18.42710 ± 0.00088	2.084598 ± 0.000044	1.179575 ± 0.00016
61–62	2862 BC – 2991 BC	38.3934 ± 0.0018	15.62077 ± 0.00062	18.40357 ± 0.00070	2.086224 ± 0.000050	1.178136 ± 0.00018
61–62*	2862 BC – 2991 BC	38.3954 ± 0.0024	15.62139 ± 0.00086	18.4043 ± 0.0010	2.086248 ± 0.000040	1.178127 ± 0.00020
63–64	3120 BC – 3239 BC	38.3920 ± 0.0020	15.62029 ± 0.00076	18.40185 ± 0.00088	2.086299 ± 0.000040	1.178064 ± 0.00016
69–70	4561 BC – 4843 BC	38.3943 ± 0.0018	15.62082 ± 0.00062	18.40950 ± 0.00076	2.085601 ± 0.000040	1.178506 ± 0.00016
75–76	6192 BC – 6434 BC	38.4279 ± 0.0026	15.62378 ± 0.00088	18.43465 ± 0.00094	2.084559 ± 0.000054	1.179899 ± 0.00020
80–81	7456 BC – 7807 BC	38.4148 ± 0.0014	15.62198 ± 0.00052	18.42193 ± 0.00072	2.085311 ± 0.000040	1.179225 ± 0.00014
87–88	8607 BC – 8678 BC	38.5019 ± 0.0020	15.63111 ± 0.00060	18.53312 ± 0.00062	2.077531 ± 0.000040	1.185636 ± 0.00020
89–90	8749 BC – 8805 BC	38.4979 ± 0.0020	15.63001 ± 0.00070	18.53026 ± 0.00066	2.077620 ± 0.000058	1.185540 ± 0.00024
100–101	9218 BC – 9259 BC	38.6691 ± 0.0040	15.65352 ± 0.00077	18.73084 ± 0.00076	2.064449 ± 0.000036	1.196604 ± 0.00016
105–106	9507 BC – 9570 BC	38.6503 ± 0.0028	15.65579 ± 0.00067	18.74324 ± 0.00074	2.06207 ± 0.000036	1.197205 ± 0.00014
108–109	9697 BC – 9760 BC	38.8640 ± 0.0036	15.68534 ± 0.00068	19.02248 ± 0.00074	2.043063 ± 0.000034	1.212753 ± 0.00012
119–120	10515 BC – 10583 BC	38.7211 ± 0.0040	15.68089 ± 0.00075	19.043 ± 0.00076	2.033391 ± 0.000034	1.21439 ± 0.00022
124–125	10848 BC – 10913 BC	38.6029 ± 0.0034	15.6539 ± 0.00060	18.75206 ± 0.00060	2.058597 ± 0.000038	1.197916 ± 0.00016

 DOI: 10.19189/MaP.2016.OMB.257

Table 3. Mass of charcoal *per* unit of volume in peat core Żyglin 3.

Depth (cm)	Peat layer boundaries calibrated mean age	Charcoal density (g dm^{-3})
20–21	AD 1088 – AD 1015	0.71
21–22	AD 1015 – AD 942	1.60
22–23	AD 942 – AD 869	1.41
23–24	AD 869 – AD 796	3.24
24–25	AD 796 – AD 723	1.38
25–26	AD 723 – AD 650	1.05
26–27	AD 650 – AD 577	1.65
27–28	AD 577 – AD 504	3.46
28–29	AD 504 – AD 422	3.70
29–30	AD 422 – AD 331	4.22
30–31	AD 331 – AD 240	2.96
31–32	AD 240 – AD 123	3.49
32–33	AD 123 –20 BC	1.48
33–34	20 BC – 163 BC	1.41
34–35	163 BC – 290 BC	0.31
35–36	290 BC – 401 BC	0.21
36–37	401 BC – 512 BC	0.077
37–38	512 BC – 623 BC	0.20
38–39	623 BC – 735 BC	0.42
39–40	735 BC – 846 BC	1.26
40–41	846 BC – 945 BC	3.52
41–42	945 BC – 1032 BC	2.43
42–43	1032 BC – 1192 BC	0.60
43–44	1192 BC – 1424 BC	0.076
44–45	1424 BC – 1580 BC	0.11
45–46	1580 BC – 1661 BC	0.80
46–47	1661 BC – 1742 BC	0.52
47–48	1742 BC – 1822 BC	0.15
48–49	1822 BC – 1903 BC	0.18
49–50	1903 BC – 1984 BC	0.73
50–51	1984 BC – 2052 BC	1.7
51–52	2052 BC – 2107 BC	1.1
52–53	2107 BC – 2162 BC	0.21
53–54	2162 BC – 2218 BC	0.012
54–55	2218 BC – 2273 BC	0.0043
55–56	2273 BC – 2328 BC	0.0019
56–57	2328 BC – 2383 BC	0.012
57–58	2383 BC – 2476 BC	1.38
58–59	2476 BC – 2604 BC	0.41
59–60	2604 BC – 2733 BC	0.32
60–61	2733 BC – 2862 BC	0.28
61–62	2862 BC – 2991 BC	1.12
62–63	2991 BC – 3120 BC	1.01
63–64	3120 BC – 3239 BC	0.31
64–65	3239 BC – 3435 BC	0.0013
65–66	3435 BC – 3717 BC	0
66–67	3717 BC – 3998 BC	0
67–68	3998 BC – 4280 BC	0
68–69	4280 BC – 4561 BC	0.022
69–70	4561 BC – 4843 BC	0
70–71	4843 BC – 5125 BC	0
71–72	5125 BC – 5406 BC	0
72–73	5406 BC – 5688 BC	0
73–74	5688 BC – 5950 BC	0.0053
74–75	5950 BC – 6192 BC	0.012
75–76	6192 BC – 6434 BC	0.012
76–77	6434 BC – 6676 BC	0
77–78	6676 BC – 6918 BC	0
78–79	6918 BC – 7160 BC	0
79–80	7160 BC – 7456 BC	0
80–81	7456 BC – 7807 BC	0
81–82	7807 BC – 8159 BC	0.0017
82–83	8159 BC – 8362 BC	0
83–84	8362 BC – 8417 BC	0
84–85	8417 BC – 8473 BC	0
85–86	8473 BC – 8536 BC	0
86–87	8536 BC – 8607 BC	0
87–88	8607 BC – 8678 BC	0.002
88–89	8678 BC – 8749 BC	0.0021
89–90	8749 BC – 8805 BC	0.0016
91–120	8846 BC – 10583 BC	0

 DOI: 10.19189/MaP.2016.OMB.257

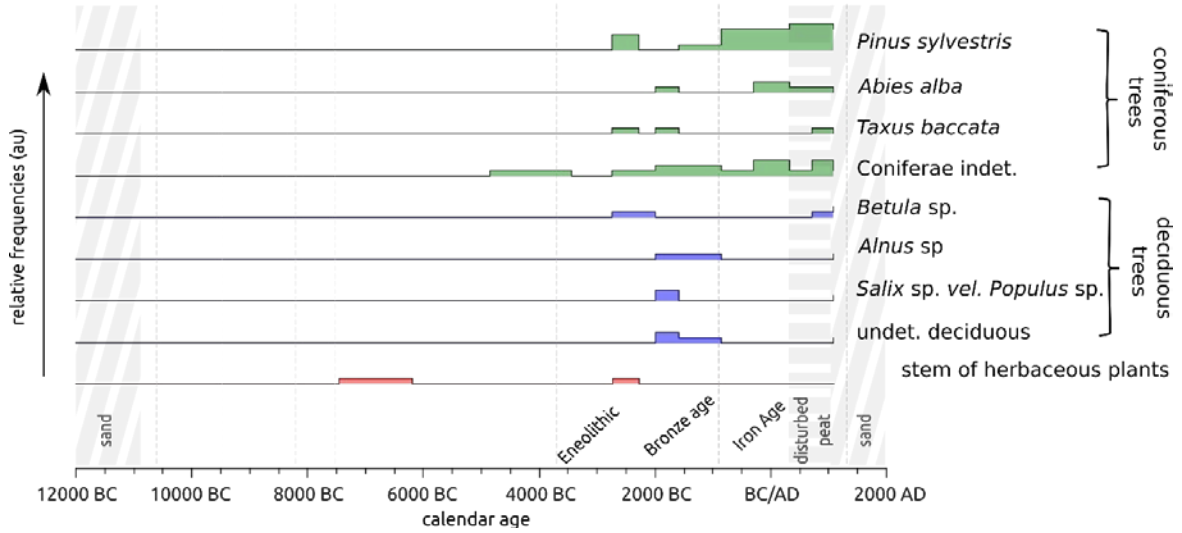

Figure 6. Results of charcoal taxonomical identification plotted on a calendar time scale.

that helps to determine the relative difference in the supply rate is the quotient of a metal (again assumed to be immobile) to a conservative element in the environment such as titanium (Ti). The changes in the metal/Ti quotient will, therefore, similarly reflect changes in the supply rate of the given metal. Quotients of Pb/Ti, Cu/Ti and Zn/Ti, with the corresponding Pb, Cu and Zn fluxes, are shown in Figure 7. The metal fluxes and metal/Ti quotients show roughly similar patterns, which is expected.

Figure 7 also contains $^{206}Pb/^{207}Pb$ quotients plotted on the calendar time scale. To decipher lead sources, isotopic quotients of $^{208}Pb/^{206}Pb$ *versus* $^{206}Pb/^{207}Pb$ are plotted in Figure 4 for 23 samples from this work. In addition, eleven ombrotrophic peat samples that correspond to the period AD 700–2000, from the work of De Vleeschouwer *et al*. (2009), are plotted in Figure 4 to give a better insight into the trend of lead isotopes. Lead ores, which are expected to contribute significantly to the lead isotopic quotient in peat, were reported for eleven galena samples from Chrzanów, Olkusz and Pomorzany (Figure 4, De Vleeschouwer *et al*. 2009). Lead isotopes from Upper Continental Crust (UCC) (estimated by Millot *et al*. 2004) are also plotted in Figure 4. The error bars in Figure 4 are substantially smaller than the symbols. In Figure 5, a 1/Pb *versus* $^{206}Pb/^{207}Pb$ binary diagram with the three periods discussed in this article is given. This shows the relationship between high lead concentration and the isotopic quotient. The temperature was retrieved from work by Davis *et al*. (2003), based on pollen studies for Western Europe. In Figure 7 this temperature is expressed as summer and winter deviations from the present-day summer and winter averages, respectively.

DISCUSSION

10700 BC to 7550 BC

The oldest peat deposits in Żyglin date back to 10700 BC and cover the beginning of the Younger Dryas. This period was significantly colder than the present (Figure 7). The initial, and by far the greatest, titanium flux values (Figure 7) match the 10600 BC (10590 ^{14}C yr BP) increase reported by other authors, for example Shotyk *et al*. (2002), who suggest that the increase was caused by specific climatic conditions. That period was characterised by increased storminess, expansion of dry, dusty areas, and reduced vegetation cover (Bond *et al*. 1997). If we are detecting the same signal in our proxies, the lead isotopic quotient should be consistent with the values for pre-anthropogenic (early Holocene) background ($^{206}Pb/^{207}Pb = 1.2045$) reported by Shotyk *et al*. (1998) and with Upper Continental Crust values (Figure 4). The mean lead isotopic quotient $^{206}Pb/^{207}Pb = 1.2052$ ($N = 4$) (Figure 4) is in good agreement with pre-anthropogenic background values, which suggests that the deposited Pb came from a distant location. If, for example, lead was transported from the surrounding areas, it would have a different isotopic fingerprint (see Figure 4 local galena ores), which is not the case here. Moreover, local soils and rocks contain significant amounts of Pb-Zn ores (Cabala *et al*. 2008, Bauerek *et al*. 2009, Smieja-Król *et al*. 2010) and our data indicate low lead flux $\Phi_{Pb} = 0.14$ mg m^{-2} yr^{-1} in 10550 BC, decreasing to 0.03 mg m^{-2} yr^{-1} ($N = 3$) from 10200 BC to 9200 BC. This is another factor which supports the hypothesis that the material did not originate from local sources. The ash content is ~10 % whereas the

Table 4. Results of the investigation of charcoal from Żyglin.

Depth (cm)	Peat layer boundaries calibrated mean age	coniferous trees				deciduous trees				stems of herbaceous plants
		Pinus sylvestris	*Abies alba*	*Taxus baccata*	Coniferae indet.	*Betula* sp.	*Alnus* sp.	*Salix* sp. vel. *Populus* sp.	undet. deciduous	
20–25	AD 1088 – AD 723	++++			+	++	+	+	+	
25–30	AD 723 – AD 331	+++++	+	+	+++	+				
30–35	AD 331 – 290 BC	+++++	+		+					
35–40	290 BC – 846 BC	++++	++		+++					
40–45	846 BC – 1580 BC	++++			+					
45–50	1580 BC – 1984 BC	+			++		+		+	
50–55	1984 BC – 2273 BC		+	+	++		+	++	++	
55–60	2273 BC – 2733 BC				+	+				
60–65	2733 BC – 3435 BC	+++		+	+	+				+
65–70	3435 BC – 4843 BC									
70–75	4843 BC – 6192 BC				+					
75–80	6192 BC – 7456 BC									
80–85	7456 BC – 8473 BC									+
85–90	8473 BC – 8805 BC									
90–95	8805 BC – 9011 BC									
95–100	9011 BC – 9218 BC									
100–105	9218 BC – 9507 BC									
105–110	9507 BC – 9823 BC									

 DOI: 10.19189/MaP.2016.OMB.257

average ash content for the rest of the core is ~ 20 %. The results indicate that the peat supply was temporarily dominated by an atmospheric input with low mineral inputs by streams. During this period no charcoal was found in peat although isopollen maps (Latałowa *et al*. 2004, Ralska-Jasiewiczowa *et al*. 2004) show a large variety of tree species, which indicates that forest fires were rather infrequent.

7550 BC to 3200 BC

The Atlantic period (7650–2900 BC) is characterised by a low peat accumulation rate (~ 0.04 mm yr^{-1}, Figure 2). This coincides with a gap in the elemental geochemistry data, which limits the interpretation. Nevertheless, it can be noted that the ash content is increasing from ~ 10 % in the previously discussed period up to ~ 20 %. This is

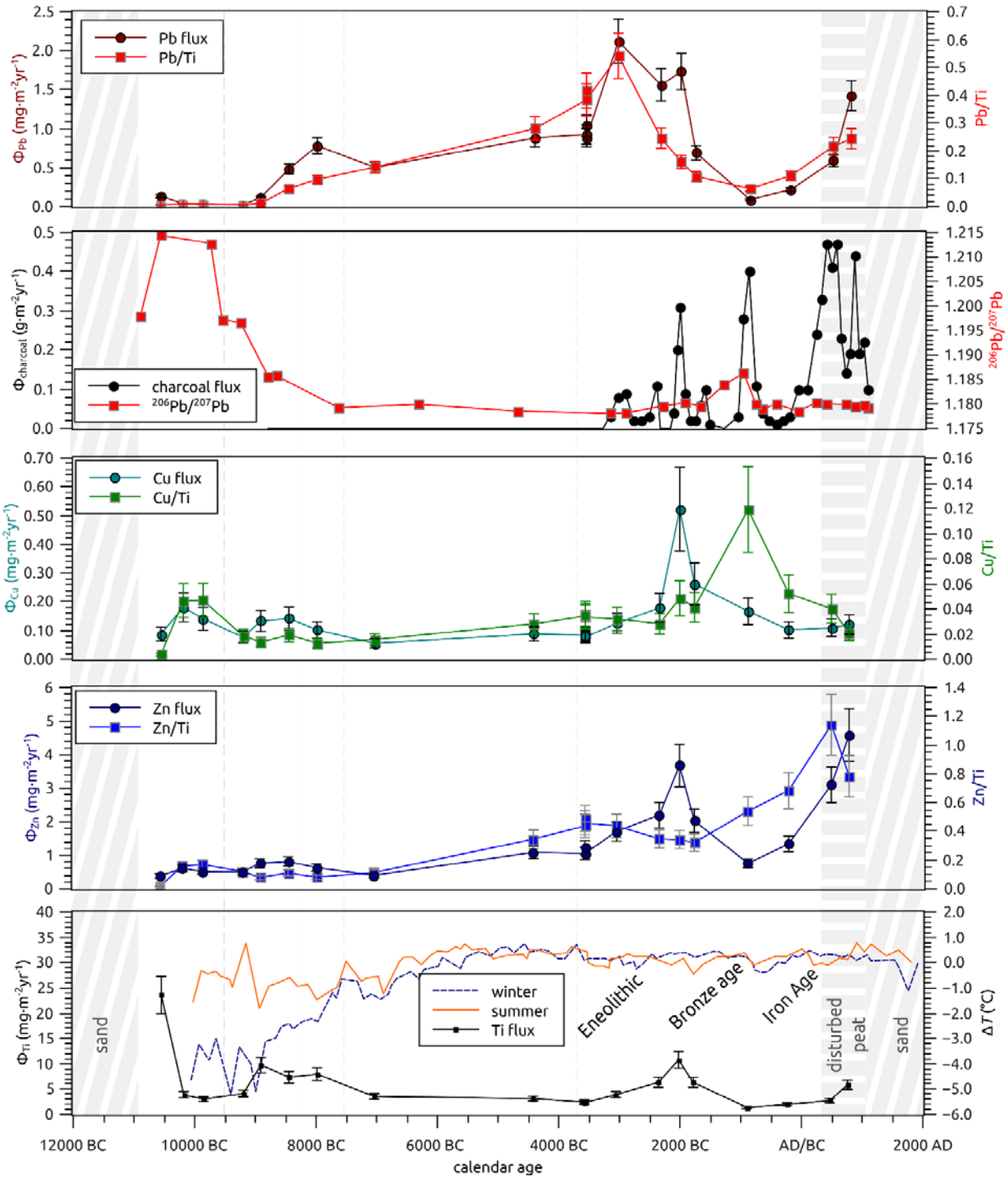

Figure 7. Fluxes of elements and charcoal, lead isotopic quotient, and reconstructed mean summer and winter temperature difference for east-central Europe during the Holocene (Davis *et al*. 2003).

most likely to be linked with the change in growth conditions of the peatland as it also affected the accumulation rate. The lead isotopic quotients shift during this period towards local galena ores (Figure 4). This indicates lead from local sources, also supported by the fact that the Pb/Ti quotient is elevated and the Pb flux reaches 1.04 mg m^{-2} yr^{-1} in 3580 BC (Figure 7). This would be expected if material was delivered from local sources rich in Pb and Zn ores. Figure 5 shows a clear lead enrichment and shift in the isotopic quotient for 7550–3200 BC data points. This confirms that local galena ore was the main source of lead in this peat deposit.

3200 BC to AD 300

Charcoal is frequently found in large amounts from 64 cm depth to the top of the peat core (Figure 7). The onset of charcoal presence corresponds to 3180 ± 80 BC, which matches the Eneolithic period. It is plausible that significant increases in charcoal content indicate human activity (e.g. Latałowa 2003, McCarroll *et al*. 2016). Natural fires may also be a cause but, surprisingly, hardly any charcoals are found below the 64th cm of the peat core (Figures 6 and 7). Hence, if natural wildfires had been the source of charcoal occurrence, it should also have been found below 64 cm depth. Moreover, taxonomical analyses (Table 4, Figure 6) indicate that coniferous trees (mainly *Pinus sylvestris*) were dominant in the anthracological spectrum. These species are particularly useful as fuel because they give a lot of dry and dead wood and are easy to harvest (Théry-Parisot 2002). The charcoal from deciduous trees like *Betula* sp., *Alnus* sp., *Populus* sp. or *Salix* sp. appears less frequently and in a later stage of the peat development. Therefore, while the possibility of natural fires cannot be ruled out, the anthracological evidence suggests that human activity influenced the abundance and composition of charcoal during this period.

Pb flux reached a maximum around 3000 BC (Φ_{Pb} = 2.12 mg m^2 yr^{-1} and Pb/Ti = 0.54), when the lead isotopes indicate that local ores were still the main source of lead. Additionally, an increase in Cu, Zn and Ti fluxes is observed around 2000 BC (Figure 7). As the heavy-metal peat contamination resulting from local smelting in the Eneolithic and Bronze Ages is expected to have been very low, it would be hard to confirm solely on the basis of metal concentration in a minerogenic peat deposit. At the same time large amounts of charcoal from deciduous and coniferous trees were also deposited in the peat (Figure 6). Therefore, the increased lead flux may be linked either to a higher erosion rate, *e.g.* due to deforestation of the surrounding area, or to early smelting activity nearby. In other parts of Europe, even earlier forest clearance and agricultural tillage have been reported. For example, in a study based on a peat core from the Swiss Jura Mountains, Shotyk *et al*. (1998, 2001) report a radiocarbon date of 5320 ^{14}C yr BP which, after radiocarbon date calibration, gives *ca*. 4150 BC.

During the investigations at Żyglin (40 m north of the Żyglin 3 core), a trunk of *Pinus silvestris* with one side charred and hollowed-out (Figure 8) was found. The calibrated radiocarbon age of this trunk is 1885–1980 BC (3580 ± 40 ^{14}C yr BP). Its origin is uncertain, but the regular shape (~ 70 × 6 × 250 cm) and very uniform charring of its inner part suggest that it is man-made, and thus independently confirms human activity in this area. An alternative but less likely explanation would be that it was charred by a wildfire and subsequently transported to the centre of the peat area by water. However, there is no evidence to support this hypothesis (*e.g.* the presence of sediment in the same peat layer).

Around 1000 BC the Pb flux reached a local minimum (0.09 mg m^2 yr^{-1}, Pb/Ti = 0.06), with a corresponding slight rise in the ^{206}Pb/^{207}Pb quotient (to 1.185) towards Upper Continental Crust values (Figure 7). The Zn and Pb fluxes, and the ^{206}Pb/^{207}Pb quotient, might point to a short and relatively small change in local conditions like an increase in vegetation cover; however, more supporting data are required. The other plausible hypothesis is a decrease in anthropic impact, which might give a similar response in our data. For example

Figure 8. Tree trunk with one side charred and hollowed-out, found in Żyglin peat (photo courtesy of M. Michnik and R. Zdaniewicz). This trunk was radiocarbon dated to 3580 ± 40 ^{14}C yr BP, and the calibrated radiocarbon age is 1885–1980 BC (using IntCal13 calibration curve).

 DOI: 10.19189/MaP.2016.OMB.257

reforestation, increase in vegetation cover and decreased usage of galena ores might cause higher $^{206}Pb/^{207}Pb$ quotient and decreased Pb and Zn fluxes.

From 500 BC to AD 300 the Pb, Zn and charcoal fluxes were rising. The most likely reason is increasing early smelting of local Ag-rich Pb-Zn ores (Molenda 1963).

AD 300 to modern times

In the uppermost part of the peat core (~ 10 cm), several charcoal pieces were found to be much younger than the peat layer in which they were located, and ^{14}C-dating outliers were detected (see Methods). Thus, the elemental geochemistry has almost certainly been altered and cannot provide a record for chronological interpretation. This is not surprising as the area has been drained twice and a sand layer now covers the peat surface. Therefore, the peat core record beyond *ca*. AD 300 would not provide reliable data and is omitted. It is important to note that, for the same location, Cabala *et al*. (2013) and Magiera *et al*. (2016) reported magnetic particles with ferri- or ferromagnetic properties and other indicators of iron ore smelting activities in the mediaeval and earlier period.

CONCLUSIONS

The investigated peat profile retrieved from Żyglin (southern Poland) corresponds to a timespan of 10700 BC to AD 500. From 10700 BC to 9000 BC the lead quotient $^{206}Pb/^{207}Pb = 1.2052$ ($N = 4$) in the peat core is consistent with values for UCC soil dust It was accompanied by a Pb flux (Figure 7) of 0.14 ± 0.02 mg m^{-2} yr^{-1} in 10550 BC, decreasing to 0.03 mg m^2 yr^{-1} ($N = 3$) from 10200 BC to 9200 BC. Local soils are highly enriched in Pb with a different isotopic composition, leading to a conclusion that the Upper Continental Crust was the main source of lead. Local soils were suppressed due to low lead flux (Figures 5 and 7).

Later (since 7550 BC), the peat accumulation rate decreased to ~ 0.04 mm yr^{-1} (Figure 2) and the lead isotopic fingerprint was identical to that of the local galena ores (Figure 4) reported by De Vleeschouwer *et al*. (2009). This indicates lead from local sources, and corresponds with a large increase in Pb flux reaching up to 1.04 ± 0.14 mg m^{-2} yr^{-1} in 3580 BC (Figure 7). From 3200 BC to AD 300 the charcoal flux (Figure 7) and, to a lesser extent, the geochemical and lead isotopic signatures indicate human activities. The first appearance of charcoal chunks *ca*. 3200 BC agrees with the generally known Eneolithic and later Bronze Age human activity in this area. The fact that almost no charcoal was found in older peat (Figures 6 and 7) makes natural fires a less likely explanation. The Pb flux reached its greatest value (2.12 ± 0.29 mg m^{-2} yr^{-1}) and, together with charcoal, may be a sign of early human activity or increased soil transport due to deforestation. Although the contamination of peat by heavy metals resulting local smelting in the Eneolithic and Bronze Ages is expected to be very low and, therefore, difficult to confirm, our data provide indications of human activity. Independent archaeological and pollen studies would provide valuable information to exclude or confirm our hypotheses. Similar investigations in neighbouring peat deposits would help to distinguish between local and global records in the peat.

ACKNOWLEDGEMENTS

Radiocarbon dating and modelling were possible thanks to own resources and BK-251 from the Institute of Physics, Silesian University of Technology. We thank Marie-Josée Tavella (EcoLab, Toulouse), Gaël Le Roux (EcoLab, Toulouse), David Baqué (EcoLab, Toulouse) and Aurélie Lanzanova (GET, Toulouse), for their help in digesting and analysing the samples for their elemental content. Lead isotopic measurements were possible thanks to a grant from WBI co-operation between Belgium and Poland. The authors are indebted to Nadine Mattielli and Jeroen de Jong for their precious assistance during the Pb isotopic analyses on the Nu Plasma MC-ICP-MS at the Laboratoire G-Time, Université Libre de Bruxelles, Belgium.

REFERENCES

Baron, S., Lavoie, M., Ploquin, A., Carignan, J., Pulido, M. & de Beaulieu, J.L. (2005) Record of metal workshops in peat deposits: history and environmental impact on the Mont-Lozère Massif (France). *Environmental Science and Technology*, 39, 5131–5140, doi: 10.1021/es048165l.

Bauerek, A., Cabala, J. & Smieja-Król, B. (2009) Mineralogical alterations of Zn-Pb flotation wastes of Mississippi Valley-type ores (southern Poland) and their impact on contamination of rainwater runoff. *Polish Journal of Environmental Studies*, 18(5), 781–788.

Bond, G., Showers, W., Cheseby, M., Lotti, R., Almasi, P., deMenocal, P., Priore, P., Cullen, H., Hajdas, I. & Bonani, G. (1997) A pervasive

 DOI: 10.19189/MaP.2016.OMB.257

millennial-scale cycle in North Atlantic Holocene and glacial climates. *Science,* 278, 1257–1266.

Bronk Ramsey, C. (2008) Deposition models for chronological records. *Quaternary Science Reviews,* 27(1–2), 42–60, doi: 10.1016/ j.quascirev.2007.01.019.

Bronk Ramsey, C. (2009) Bayesian analysis of radiocarbon dates. *Radiocarbon,* 51(1), 337–360.

Cabala, J., Smieja-Król, B., Jablonska, M. & Chrost, L. (2013). Mineral components in a peat deposit: looking for signs of early mining and smelting activities in Silesia-Cracow region (Southern Poland). *Environmental Earth Sciences,* 69(8), 2559–2568, doi: 10.1007/s12665-012-2080-6.

Cabala, J., Zogala, B. & Dubiel, R. (2008) Geochemical and geophysical study of historical Zn-Pb ore processing waste dump areas (Southern Poland). *Polish Journal of Environmental Studies,* 17(5), 693–700.

Chróst, L. (2013) Ołowiowy ślad "Wiślan" odczytany z torfowisk obszaru kruszconośnego śląsko-małopolskiego (Lead mark of Vistulians tribe recorded in a peat bog in Silesia-Little Poland). In: Broń, P. (ed.) *Argenti Fossores et Alii* (*Silver Miners and Others*), Chronicon, Wrocław, 175–185 (in Polish).

Chróst, L., Kandzia, M. & Wasielewski, R. (2007) *Określenie intensywności dawnej produkcji srebra i ołowiu w rejonie Tarnowskich Gór w oparciu o pomiary depozycji ołowiu w torfowiskach* (*Estimation of the Intensity of Early Silver and Lead Production in Tarnowskie Góry Region, Poland, Based on the Deposition of Lead Recorded in Peat Bogs*). Report, Public Procurement Project, Wydział Kultury Urzędu Marszałkowskiego Województwa Śląskiego (Culture Department, The Marshal's office of Silesian Voivodeship) and Stowarzyszenie Miłośników Ziemi Tarnogórskiej (Society of Friends of the Tarnowskie Góry Land), Katowice and Tarnowskie Góry, 52 pp. (in Polish).

Chróst, L., Kandzia, M. & Wasielewski, R. (2008) *Określenie usytuowania w rejonie Tarnowskich Gór ośrodków wczesnośredniowiecznego hutnictwa ołowiu i srebra metodą pomiarów lokalnego skażenia torfowisk i gleb ołowiem* (*Localization of the Early Mediaeval Silver-lead Smelting Centres in the Area of Tarnowskie Gory, Poland, Based on the Determination of the Lead Contamination of Soil and Peat*). Public Procurement Project Report, Wydział Kultury Urzędu Marszałkowskiego Województwa Śląskiego (Culture Department, The Marshal's office of Silesian Voivodeship) and Stowarzyszenie Miłośników Ziemi Tarnogórskiej (Society of Friends of the Tarnowskie Góry Land), Katowice and Tarnowskie Góry, 38pp. (in Polish).

Davis, B.A., Brewer, S., Stevenson, A.C. & Guiot, J. (2003) The temperature of Europe during the Holocene reconstructed from pollen data. *Quaternary Science Reviews,* 22, 1701–1716, doi: 10.1016/S0277-3791(03)00173-2.

De Vleeschouwer, F., Fagel, N., Cheburkin, A., Pazdur, A., Sikorski, J., Mattielli, N., Renson, V., Fialkiewicz, B., Piotrowska, N. & Le Roux, G. (2009) Anthropogenic impacts in North Poland over the last 1300 years — A record of Pb, Zn, Cu, Ni and S in an ombrotrophic peat bog. *Science of The Total Environment,* 407(21), 5674–5684, doi: 10.1016/j.scitotenv.2009.07.020.

De Vleeschouwer, F., Gérard, L., Goormaghtigh, C., Mattielli, N., Le Roux, G. & Fagel, N. (2007) Atmospheric lead and heavy metal pollution records from a Belgian peat bog spanning the last two millennia: Human impact on a regional to global scale. *Science of The Total Environment,* 377(2–3), 282–295, doi: 10.1016/j.scitotenv. 2007.02.017.

De Vleeschouwer, F., Pazdur, A., Luthers, C., Streel, M., Mauquoy, D., Wastiaux, C., Le Roux, G., Moschen, R., Blaauw, M., Pawlyta, J., Sikorski, J. & Piotrowska, N. (2012) A millennial record of environmental change in peat deposits from the Misten bog (East Belgium). *Quaternary International,* 268, 44–57, doi: 10.1016/j.quaint.2011.12.010.

Drabina, J. (2000) *Historia Tarnowskich Gór* (*History of Tarnowskie Góry*). Museum of Tarnowskie Góry, Tarnowskie Góry, 797 pp., ISBN 83-911508-3-6 (in Polish).

Lamentowicz, M., Balwierz, Z., Forysiak, J., Płóciennik, M., Kittel, P., Kloss, M., Twardy, J., Żurek, S. & Pawlyta, J. (2009) Multiproxy study of anthropogenic and climatic changes in the last two millennia from a small mire in central Poland. *Hydrobiologia,* 631(1), 213–230, doi: 10.1007/s10750-009-9812-y.

Latałowa, M. (2003) Holocen (Holocene). In: Dybova-Jachowicz, S. & Sadowska, A. (eds.) *Palinologia* (*Palynology*). W. Szafer Institute of Botany, Polish Academy of Sciences, Kraków, 273–307 (in Polish).

Latałowa, M., Tobolski, K. & Nalepka, D. (2004) *Pinus* L. subgenus *Pinus* (subgen. *Diploxylon* (Koehne) Pilger) - Pine. In: Ralska-Jasiewiczowa, M., Latałowa, M., Wasylikowa, K., Tobolski, K., Madejska, E., Wright, H.E.Jr. & Turner, C. (eds.) *Late Glacial and Holocene History of Vegetation in Poland Based on Isopollen Maps*. W. Szafer Institute of Botany,

 DOI: 10.19189/MaP.2016.OMB.257

Polish Academy of Sciences, Kraków, 165–177.

Le Roux, G. & De Vleeschouwer, F. (2010) Preparation of peat samples for inorganic geochemistry used as palaeoenvironmental proxies. *Mires and Peat*, 7(04), 1–9.

Leach, D.L. & Viets, J.G. (1992) *Comparison of the Cracow-Silesian Mississippi Valley-type District, Southern Poland, with Mississippi Valley-type Districts in North America*. Report OF/92-704, United States Department of the Interior U.S. Geological Survey, 74 pp.

Leach, D.L. & Viets, J.G. (1993) A preliminary comparison of the Silesian-Cracow Mississippi Valley-type district (southern Poland) with Mississippi Valley-type districts in North America. *Geological Quarterly*, 37(2), 325–328.

Lityńska-Zając, M. & Wasylikowa, K. (2005) *Przewodnik do Badań Archeobotanicznych* (*Archaeobotanical Research Guidebook*). Vademecum Geobotanicum Series (ed. J.B. Faliński), Sorus, Poznań, 568 pp. (in Polish).

Magiera, T., Mendakiewicz, M., Szuszkiewicz. M., Jabłońska. M. & Chróst, L. (2016) Technogenic magnetic particles in soils as evidence of historical mining and smelting activity: A case of the Brynica River Valley, Poland. *Science of The Total Environment*, 566–567, 536–551, doi: 10.1016/j.scitotenv.2016.05.126.

McCarroll, J., Chambers, F.M., Webb, J.C. & Thom, T. (2016) Informing innovative peatland conservation in light of palaeoecological evidence for the demise of *Sphagnum imbricatum*: the case of Oxenhope Moor, Yorkshire, UK. *Mires and Peat*, 18(08), 1–24, doi: 10.19189/MaP.2015.OMB.206.

Millot, R., Allègre, C.J., Gaillardet, J. & Roy, S. (2004) Lead isotopic systematics of major river sediments: a new estimate of the Pb isotopic composition of the Upper Continental Crust. *Chemical Geology*, 203(1–2), 75–90, doi: 10.1016/j.chemgeo.2003.09.002.

Molenda, D. (1963) *Górnictwo Kruszcowe na Terenie Złóż Śląsko-Krakowskich do Połowy XVI Wieku* (*Mining Ore Deposits in the Silesian-Cracow to the Mid-sixteenth Century*). Studia Dziejów Górnictwa i Hutnictwa (Studies in the History of Mining and Metallurgy), Volume 8, Polish Academy of Sciences, Ossolineum Wrocław-Warszawa-Kraków,187–198(in Polish).

Nichols, G.J., Cripps, J.A., Collinson, M.E. & Scott, A.C. (2000) Experiments in waterlogging and sedimentology of charcoal: Results and implications. *Palaeogeography, Palaeoclimatology, Palaeoecology*, 164(1–4), 43–56.

NID (2014) National Heritage Board of Poland database. Online at: http://geoportal.nid.pl/nid/

Novak, M. & Pacherova, P. (2008) Mobility of trace metals in pore waters of two Central European peat bogs. *Science of The Total Environment*, 394, 2–3, 331–337, doi: 10.1016/j.scitotenv.2008.01.036.

Pawlyta, J., Pazdur, A., Rakowski, A., Miller, B.F. & Harkness, D.D. (1998) Commissioning of Quantulus 1220™ liquid scintillation beta spectrometer for measuring ^{14}C and ^{3}H at natural abundance levels. *Radiocarbon,* 40(1), 201–209.

Ralska-Jasiewiczowa, M., Latałowa, M., Wasylikowa, K., Tobolski, K., Madejska, E., Wright, H.E.Jr. & Turner, C. (eds.) (2004) *Late Glacial and Holocene History of Vegetation in Poland Based on Isopollen Maps*. W. Szafer Institute of Botany, Polish Academy of Sciences, Kraków, 444 pp.

Reimer, P.J., Bard, E., Bayliss, A., Beck, J.W., Blackwell, P.G., Bronk Ramsey, C., Grootes, P.M., Guilderson, T.P., Haflidason, H., Hajdas, I., Hatte, C., Heaton, T.J., Hoffmann, D.L., Hogg, A.G., Hughen, K.A., Kaiser, K.F., Kromer, B., Manning, S.W., Niu, M., Reimer, R.W., Richards, D.A., Scott, E.M., Southon, J.R., Staff, R.A., Turney, C.S.M. & van der Plicht, J. (2013) IntCal13 and Marine13 Radiocarbon Age Calibration Curves 0–50,000 Years cal BP. *Radiocarbon*, 55(4), 1869–1887, doi: 10.2458/azu_js_rc.55.16947.

Renson, R., Fagel, N., Mattielli, N., Nekrassoff, S., Streel, M. & De Vleeschouwer, F. (2008) Roman road pollution assessed by elemental and lead isotope geochemistry in East Belgium. *Applied Geochemistry*, 23(12), 3253–3266, doi: 10.1016/j.apgeochem.2008.06.010.

Schweingruber, F.H. (1978) *Mikroskopische Holzanatomie* (*Microscopic Wood Anatomy*). Eidgenössische Anstalt für das forstliche Versuchswesen, Kommissionsverlag Zürcher AG, Zug, 312 pp. (in German).

Schweingruber, F.H. (1990) *Anatomie europäischer Hölzer. Ein Atlas zur Bestimmung europäischer Baum-, Strauch und Zwergstrauchhölzer* (*Anatomy of European Wood. An Atlas for European Trees, Shrubs and Dwarf Shrubs*). Verlag Paul Haupt, Bern-Stuttgart, 800 pp. (in German).

Scott, A.C. (2010) Charcoal recognition, taphonomy and uses in palaeoenvironmental analysis. *Palaeogeography, Palaeoclimatology, Palaeoecology*, 291(1–2), 11–39, doi: 10.1016/j.palaeo.2009.12.012.

Shotyk, W., Blaser, P., Grünig, A. & Cheburkin, A.K. (2000) A new approach for quantifying

 DOI: 10.19189/MaP.2016.OMB.257

cumulative, anthropogenic, atmospheric lead deposition using peat cores from bogs: Pb in eight Swiss peat bog profiles. *Science of The Total Environment*, 249(1–3), 281–295, doi: 10.1016/S0048-9697(99)00523-9.

Shotyk, W., Krachler, M., Martinez-Cortizas, A., Cheburkin, A.K. & Emons, H. (2002) A peat bog record of natural, pre-anthropogenic enrichments of trace elements in atmospheric aerosols since 12 370 ^{14}C yr BP, and their variation with Holocene climate change. *Earth and Planetary Science Letters*, 199(1–2), 21–37, doi: 10.1016/S0012-821X(02)00553-8.

Shotyk, W., Weiss, D., Appleby, P.G., Cheburkin, A.K., Frei, R., Gloor, M., Kramers, J.D., Reese, S. & Van Der Knaap, W.O. (1998) History of atmospheric lead deposition since 12,370 ^{14}C yr BP from a peat bog, Jura Mountains, Switzerland. *Science*, 281(5383), 1635–1640, doi: 10.1126/science.281.5383.1635.

Shotyk, W., Weiss, D., Kramers, J.D., Frei, R., Cheburkin, A.K., Gloor, M. & Reese, S. (2001) Geochemistry of the peat bog at Etang de la Gruère, Jura Mountains, Switzerland, and its record of atmospheric Pb and lithogenic trace metals (Sc, Ti, Y, Zr, and REE) since 12,370 ^{14}C yr BP. *Geochimica et Cosmochimica Acta*, 65(14), 2337–2360, doi: 10.1016/S0016-7037(01)00586-5.

Smieja-Król, B., Fiałkiewicz-Kozieł, B., Sikorski, J. & Palowski, B. (2010) Heavy metal behaviour in peat - A mineralogical perspective. *Science of The Total Environment*, 408(23), 5924–5931, doi: 10.1016/j.scitotenv.2010.08.032.

Stuiver, M. & Polach, H.A. (1977) Discussion: reporting of ^{14}C data. *Radiocarbon*, 19(3), 355–363.

Theodórsson, P. (2005) A simple, extremely stable single-tube liquid scintillation system for radiocarbon dating. *Radiocarbon*, 47(1), 89–97.

Théry-Parisot, I. (2002) Gathering of fire wood during the Palaeolithic. In: Thiébault, S. (ed.) *Charcoal Analysis. Methodological Approaches, Palaeoecological Results and Wood Uses*, Proceedings of the Second International Meeting of Anthracology, Paris, September 2000. BAR International Series, 1063, 243–249.

Tudyka, K. & Pazdur, A. (2010) Radiocarbon dating of peat profile with metallurgy industry evidence. *Geochronometria*, 35(1), 3–9, doi: 10.2478/v10003-010-0007-3.

Tudyka, K. & Pazdur, A. (2012) ^{14}C dating with the ICELS liquid scintillation counting system using fixed-energy balance counting window method. *Radiocarbon*, 54(2), 267–273, doi: 10.2458/azu_js_rc.v54i2.15832.

Weis, D., Kieffer, B., Maerschalk, C., Pretorius, W. & Barling, J. (2005) High-precision Pb-Sr-Nd-Hf isotopic characterization of USGS BHVO-1 and BHVO-2 reference materials. *Geochemistry, Geophysics, Geosystems*, 6(2), Q02002.

Weiss, D., Shotyk, W., Kramers, J.D. & Gloor, M. (1999) *Sphagnum* mosses as archives of recent and past atmospheric lead deposition in Switzerland. *Atmospheric Environment*, 33(23), 3751–3763, doi: 10.1016/S1352-2310(99)00093-X.

Submitted 26 Sep 2016, revision 10 Feb 2017
Editor: Olivia Bragg

Author for correspondence: Konrad Tudyka, Department of Radioisotopes, Institute of Physics - Centre for Science and Education, Silesian University of Technology, Konarskiego 22B, 44-100 Gliwice, Poland
Email: konrad.tudyka@polsl.pl

 DOI: 10.19189/MaP.2016.OMB.257

Appendix

Table A1. ^{14}C dates by layer of a peat profile from Żyglin site obtained on three different spectrometers, after Tudyka & Pazdur (2010, 2012). For the deepest layer (125–127.5 cm), sample age (*) is 1160 ^{14}C yr younger than the erroneous result published by Tudyka & Pazdur (2010), which was revised after we noticed a systematic decrease of standard count rate caused by a sample elevator breakdown in the Quantulus 1220™.

Depth (cm)	Spectrometer	Lab. no.	Radiocarbon age (14C yr BP)
20–21	Quantulus 1220™ no. 2	GdS-759	1410 ± 55
22–23	ICELS no. 2	GdC-244	1270 ± 130
28–29	ICELS no. 1	GdC-565	1560 ± 40
	ICELS no. 2	GdC-564	1565 ± 50
	Quantulus 1220™ no. 2	GdS-848	1660 ± 50
29–30	ICELS no. 1	GdC-563	2045 ± 70
	ICELS no. 2	GdC-566	2030 ± 50
	Quantulus 1220™ no. 2	GdS-849	1990 ± 65
31–32	ICELS no. 1	GdC-419	1755 ± 70
	ICELS no. 2	GdC-418	1795 ± 75
	Quantulus 1220™ no. 2	GdS-850	1830 ± 55
31–32	ICELS no. 1	GdC-419	1755 ± 70
	ICELS no. 2	GdC-418	1795 ± 75
	Quantulus 1220™ no. 2	GdS-850	1830 ± 55
34–35	ICELS no. 1	GdC-557	2310 ± 160
	ICELS no. 2	GdC-556	2230 ± 200
	Quantulus 1220™ no. 2	GdS-859	2210 ± 150
40–41	ICELS no. 1	GdC-561	2715 ± 50
	ICELS no. 2	GdC-560	2720 ± 40
	Quantulus 1220™ no. 2	GdS-858	2915 ± 55
42–43	ICELS no. 1	GdC-569	2770 ± 70
	ICELS no. 2	GdC-572	2870 ± 55
	Quantulus 1220™ no. 2	GdS-834	2910 ± 50
44–45	Quantulus 1220™ no. 2	GdS-851	3315 ± 50
50–51	Quantulus 1220™ no. 2	GdS-830	3695 ± 50
57–58	ICELS no. 1	GdC-417	3960 ± 70
	ICELS no. 2	GdC-420	3780 ± 50
	Quantulus 1220™ no. 2	GdS-835	3865 ± 50

 DOI: 10.19189/MaP.2016.OMB.257

Depth (cm)	Spectrometer	Lab. no.	Radiocarbon age (14C yr BP)
63–64	ICELS no. 1	GdC-409	4400 ± 100
	ICELS no. 2	GdC-412	4500 ± 55
	Quantulus 1220™ no. 2	GdS-763	4445 ± 90
64–65	ICELS no. 1	GdC-411	4550 ± 110
	ICELS no. 2	GdC-410	4590 ± 50
	Quantulus 1220™ no. 2	GdS-760	4435 ± 65
73–74	Quantulus 1220™ no. 2	GdS-873	6945 ± 70
79–80	ICELS no. 1	GdC-427	8300 ± 130
	ICELS no. 2	GdC-412	8130 ± 70
	Quantulus 1220™ no. 2	GdS-874	8340 ± 75
82–83	Quantulus 1220™ no. 2	GdS-884	9265 ± 70
85–86	ICELS no. 1	GdC-243	9120 ± 80
	Quantulus 1220™ no. 2	GdS-875	9320 ± 80
89–90	ICELS no. 1	GdC-559	9570 ± 100
	ICELS no. 2	GdC-562	9460 ± 110
	Quantulus 1220™ no. 2	GdS-876	9740 ± 110
92.5–95	ICELS no. 1	GdC-431	9950 ± 100
	ICELS no. 2	GdC-430	9600 ± 200
	Quantulus 1220™ no. 2	GdS-1054	10090 ± 140
100–102.5	ICELS no. 1	GdC-429	9890 ± 120
	ICELS no. 2	GdC-432	9740 ± 65
	Quantulus 1220™ no. 2	GdS-1055	9785 ± 110
110–112.5	ICELS no. 1	GdC-478	10100 ± 100
	ICELS no. 2	GdC-479	10110 ± 95
	Quantulus 1220™ no. 2	GdS-1057	9950 ± 120
115–117.5	ICELS no. 1	GdC-555	10710 ± 190
	ICELS no. 2	GdC-558	10525 ± 55
	Quantulus 1220™ no. 2	GdS-1057	10210 ± 110
120–122.5	ICELS no. 1	GdC-477	10620 ± 100
	ICELS no. 2	GdC-580	10640 ± 65
	Quantulus 1220™ no. 2	GdS-1058	10660 ± 110
125–127.5	Quantulus 1220™ no. 2	GdS-896	10880 ± 110*

 DOI: 10.19189/MaP.2016.OMB.257